SF2A 2008
C. Charbonnel, F. Combes and R. Samadi (eds)

STOCHASTIC MODEL OF ACCELERATION TO ULTRA HIGH ENERGY

Fraschetti, F.[1]

Abstract. In the past year, the HiRes and Auger collaborations have reported the discovery of a high-energy cutoff in the ultra-high-energy cosmic-ray (UHECR) spectrum, and an apparent clustering of the highest energy events towards nearby active galactic nuclei (AGNs). Consensus is building that such 10^{19}-10^{20} eV particles are accelerated within the radio-bright lobes of these sources, but it is not yet clear how this actually happens. We report (to our knowledge) the first treatment of particle acceleration in such environments from first principles, showing that energies of order 10^{20} eV are reached in 10^7 years for protons. This prediction appears to be consistent with the Auger observations. However, our findings reopen the question regarding whether the high-energy cutoff is due solely to propagation effects, or whether it represents the maximum energy permitted by the acceleration process itself.

1 Introduction

The understanding of the origin of Ultra-High-Energy Cosmic Rays (UHECRs) still represents one the major challenges of theoretical astrophysics. Recently the observations by Pierre Auger Observatory (PAO), demonstrating a low fraction of high-energy photons in the Cosmic Ray distribution, rule out the top-down models, in which the UHECRs represent the decay products of high-mass particles created in the early Universe (Semikoz et al. 2007). The measured photon flux is also in conflict with scenarios in which UHECRs are produced by collisions between cosmic strings or topological defects (Bluemer et al 2008; Auger 2008b). On the other hand, such extremely energetic particles may still be produced via astrophysical acceleration mechanisms (Fraschetti 2008; Torres & Anchordoqui 2004 and other references cited therein).

Moreover the long sought GZK cutoff (Greisen 1966; Zatsepin & Kuz'min 1966) in Cosmic Ray spectrum due to interactions of primary protons with the CMB has been claimed to have been observed by the High Resolution Fly's Eye (Abbasi et al. 2008). A spectral steepening at the expected energy $E_{GZK} \sim 4 \times 10^{19}$ eV has also been observed by PAO (Auger 2008c).

The PAO has confirmed that active galactic nuclei (AGN) located within ~ 75 Mpc are correlated with the arrival directions of UHECRs (Auger 2008a). However, the question remains open regarding the mechanism of acceleration to such high energies and the origin of the observed cutoff in the spectrum, i.e., whether it is due solely to the GZK effect, or it also points to an intrinsic limit to the acceleration efficiency.

UHECRs generation scenarios include the so-called first-order Fermi acceleration in GRBs, Pulsar Wind Bubbles, and also relativistic second order Fermi acceleration (Fermi 1949). We report here a treatment of propagation and acceleration of individual particle in the lobes of radio-bright AGNs from first principles (Fraschetti & Melia 2008), considering the acceleration of charged particles via random scatterings (a second-order process) with fluctuations in a turbulent magnetic field.

2 Model of magnetic turbulence

In our treatment, we follow the three-dimensional motion of *individual* particles within a time-varying field. By avoiding the use of equations describing statistical averages through the phase space distribution function of a given population of particles, we mitigate our dependence on unknown factors, such as the diffusion coefficient. We also avoid the need to use the Parker approximation (Padmanabhan 2001) in the transport equation. For

[1] LUTh, Observatoire de Paris, CNRS-UMR8102 and Université Paris VII, 5 Place Jules Janssen, F-92195 Meudon Cédex, France

simplicity, we assume that the magnetic energy is divided equally between the two components: background and turbulence; the actual value of this fraction does not produce any significant qualitative differences in our results. For many real astrophysical plasmas, the magnetic turbulence seems to be in accordance with the Kolmogorov spectrum; a more recent numerical analysis of MHD turbulence confirms the general validity of the Kolmogorov power spectrum (Cho et al. 2003). In addition, renormalization group techniques applied to the analysis of MHD turbulence also favour a Kolmogorov power spectrum (for more details, see Verma 2004).

We calculate the trajectory of a test particle with charge e and mass m in a magnetic field $\mathbf{B}(t,\mathbf{r}) = mc\mathbf{\Omega}(t,\mathbf{r})/e$, where c is the speed of light in vacuum. The particle motion is obtained as a solution of the Lorentz equation

$$\frac{d\mathbf{u}(t)}{dt} = \delta\mathcal{E}(t,\mathbf{r}) + \frac{\mathbf{u}(t)\times\mathbf{\Omega}(t,\mathbf{r})}{\gamma(t)} \ , \tag{2.1}$$

where $\mathbf{u}$ is the three-space vector of the four-velocity $u^\mu = (\gamma, \gamma\mathbf{v}/c)$, t is the time in the rest frame of the source, and γ is the Lorentz factor $\gamma = 1/\sqrt{1-(v/c)^2}$. The quantity $\mathbf{\Omega}$ in equation (2.1) is given by $\mathbf{\Omega}(t,\mathbf{r}) = \mathbf{\Omega}_0 + \delta\mathbf{\Omega}(t,\mathbf{r})$, where $\mathbf{\Omega}_0 = e\mathbf{B}_0/mc$ and $\mathbf{B}_0$ is the background magnetic field. The time variation of the magnetic field, however, induces an electric field $\delta\mathcal{E}(t,\mathbf{r}) = (e/mc)\mathbf{E}(t,\mathbf{r})$ according to Faraday's law. We ignore any large-scale background electric fields; this is a reasonable assumption given that currents would quench any such fields within the radio lobes of AGNs.

We follow the prescription of (Giacalone & Jokipii 1994) for generating the turbulent magnetic field, including a time-dependent phase factor to allow for temporal variations. The procedure of building the turbulence calls for the random generation of a given number N of transverse waves $\mathbf{k}_i$, $i = 1, .., N$ at every point of physical space where the particle is found, each with a random amplitude, phase and orientation defined by angles $\theta(k_i)$ and $\phi(k_i)$. This form of the fluctuation satisfies $\nabla\cdot\delta\mathbf{\Omega}(t,\mathbf{r}) = 0$. We write

$$\delta\mathbf{\Omega}(t,\mathbf{r}) = \sum_{i=1}^{N} \Omega(k_i)\hat{\xi}_{\pm}(k_i) e^{\left[i(k_i x' - \omega_i t + \beta(k_i))\right]} \ , \tag{2.2}$$

where the polarization vector is given by

$$\hat{\xi}_{\pm}(k_i) = \cos\alpha(k_i)\hat{\mathbf{y}}' \pm i\sin\alpha(k_i)\hat{\mathbf{z}}' \ . \tag{2.3}$$

The primed reference system (x', y', z') is related to the lab-frame coordinates (x, y, z) via a rotation in terms of $\theta(k_i)$ and $\phi(k_i)$ (Fraschetti & Melia 2008). For each k_i, there are 5 random numbers: $0 < \theta(k_i) < \pi$, $0 < \phi(k_i) < 2\pi$, $0 < \alpha(k_i) < 2\pi$, $0 < \beta(k_i) < 2\pi$ and the sign $\pm$ indicating the sense of polarization. We use the dispersion relation for transverse non-relativistic Alfven waves in the background plasma: $\omega(k_i) = v_A k_i cos\theta(k_i)$, where $v_A = B_0/\sqrt{4\pi m_p n}$ is the non-relativistic Alfven velocity in a medium with background magnetic field B_0 and number density n, being m_p the proton mass, and $\theta(k_i)$ is the angle between the wavevector k_i and B_0. The background plasma is assumed to have a background number density $n \sim 10^{-4}$ cm^{-3}, a reasonable value for the radio lobes of AGNs.

The amplitudes of the magnetic fluctuations are assumed to be generated by Kolmogorov turbulence, so

$$\Omega(k_i) = \Omega(k_{min})\left(\frac{k_i}{k_{min}}\right)^{-\Gamma/2} \ , \tag{2.4}$$

where k_{min} corresponds to the longest wavelength of the fluctuations and $\Gamma = 5/3$. Finally, the quantity $\Omega(k_{min})$ is computed by requiring that the energy density of the magnetic fluctuations equals that of the background magnetic field: ${B_0}^2/8\pi$.

We choose N=2400 values of k evenly spaced on a logarithmic scale; considering that the turbulence wavenumber k is related to the turbulent length scale l by $k = 2\pi/l$, we adopt a range of lengthscales from $l_{min} = 10^{-1}\, v_0/\Omega_0$ to $l_{max} = 10^9\, v_0/\Omega_0$, where v_0 is the initial velocity of the particle and Ω_0 is its gyrofrequency in the background magnetic field. Thus the dynamic range covered by k is $k_{max}/k_{min} = l_{max}/l_{min} = 10^{10}$ and the interaction of particle with the turbulent waves is gyroresonant at all times. The particles propagating through this region are released at a random position inside the acceleration zone, which for simplicity is chosen to be a sphere of radius $\mathcal{R}$, with a fixed initial velocity u_0 pointed in a random direction. The initial value of the Lorentz factor $\gamma_0 = \sqrt{1+{u_0}^2} \sim 1.015$ is chosen to avoid having to deal with ionization losses for the protons.

Assuming that both the radio and CMB intensity fields are isotropic, we take these energy losses into account using the following angle-integrated power-loss rate:

$$-\frac{dE}{dt} = \frac{4}{3}\sigma_T(m)c\gamma^2\left(\frac{B^2}{8\pi} + U_R + U_{CMB}\right) , \quad (2.5)$$

where $\sigma_T(m) = 6.6524 \times (m_e/m)^2\, 10^{-25}$ cm^2 is the Thomson cross section for a particle of mass m, $B^2/(8\pi) = (2{B_0}^2)/(8\pi)$ is the total energy density of the magnetic field, and U_R is the photon energy density inside a typical Radio Lobe, for which we assume a standard luminosity density corresponding to the Fanaroff-Riley class II of galaxies (with a luminosity $L = 5 \times 10^{25}$ W Hz^{-1} sr^{-1} at 178 MHz), and $\mathcal{R}$ is the radius of the acceleration zone. For the CMB, we use $U_{CMB} = aT^4 = 4.2 \times 10^{-13}$ erg cm^{-3}. In Fig. 1, we plot the time evolution of the particle Lorentz factor γ for three representative values of the background field B_0: 10^{-7}, 10^{-8}, and 10^{-9} gauss. We see the particle undergoing various phases of acceleration and deceleration as it encounters fluctuations in **B**.

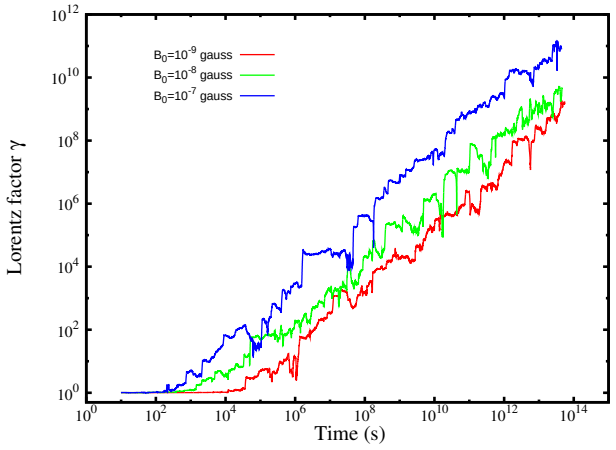

Fig. 1. Simulated time evolution of the Lorentz factor γ for a proton propagating through a time-varying turbulent magnetic field. The particle is followed until it leaves the acceleration zone and enters the intergalactic medium. The acceleration timescale Δt is inversely proportional to the background field B_0. Therefore, as expected, a larger B_0 produces a more efficient acceleration.

In a region where magnetic turbulence is absent or static, a given test particle propagates by "bouncing" randomly off the inhomogeneities in **B**, but its energy remains constant. The field we are modeling here, however, is comprised of transverse plane waves (see equation 2.2), and collisions between the test particle and these waves produces (on balance) a net acceleration as viewed in the lab frame. A sampling of parameter space is shown in Fig. 2.

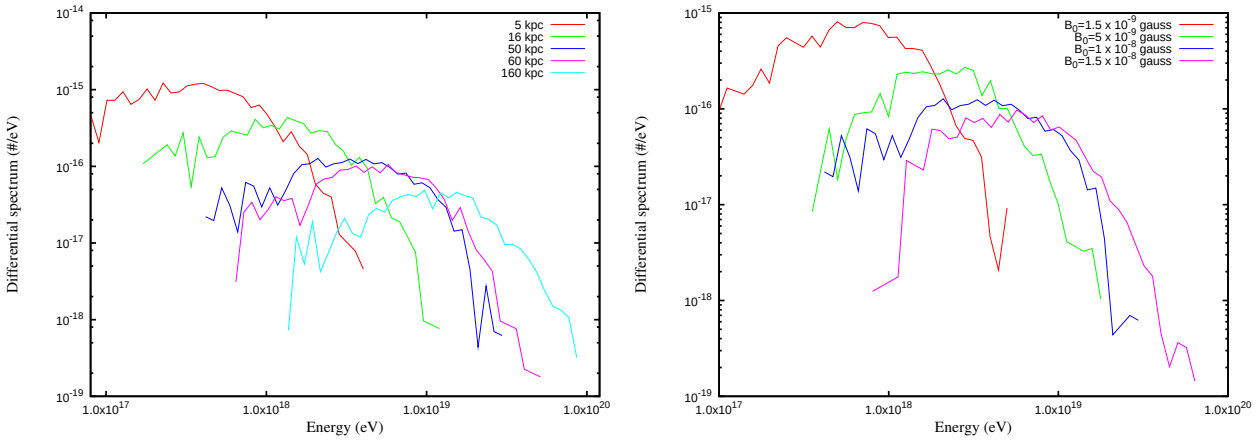

Fig. 2. Left: Calculated differential spectra for 500 protons with $B_0 = 10^{-8}$ gauss and for different values of the size of the acceleration region, assumed to be a sphere of radius spanning the interval $\mathcal{R} = [5 - 160]$ kpc. The dependence of the energy cutoff on $\mathcal{R}$ is evidenced. This result shows that the cutoff in the observed spectral distribution can be due to the competition between two distint effects: propagation through the CMB and intrinsic properties of the accelerator. Moreover, the slope in the region $E > 4 \times 10^{18}$ eV strongly depends on R. This diagram supports the view that the steeper CR spectrum below $\log(E/eV) \approx 18.6$ likely represents a population of galactic cosmic rays. **Right:** Calculated differential spectra for 500 protons with $R = 50$ kpc and for different values of the turbulent magnetic energy. In this case B_0 spans the interval $B_0 = 1.5 \times [10^{-9} - 10^{-8}]$ gauss.

In Fig. 3, we compare a theoretical differential injection spectrum for a population of 1,000 protons with energy $E > 4 \times 10^{18}$ eV with a power law in arbitrary units of index -2.6. We infer that for a radius $\mathcal{R} = 50$ kpc, B_0 should lie in the range $[0.5 - 5] \times 10^{-8}$ gauss. The observed spectrum may be affected by the cosmological evolution in source density. However, a likelihood analysis (Gelmini et al 2007) of the dependence of the observed distribution on input parameters has already shown that, in the case of pure proton-fluxes of primaries, for $\alpha \sim 0$, where α is the evolution index in the source density, the HiRes observations are compatible with a power-law injection spectrum with index -2.6 (Fraschetti & Melia 2008). Thus, in a more conservative interpretation, the result presented here provides the injection spectrum from a single source.

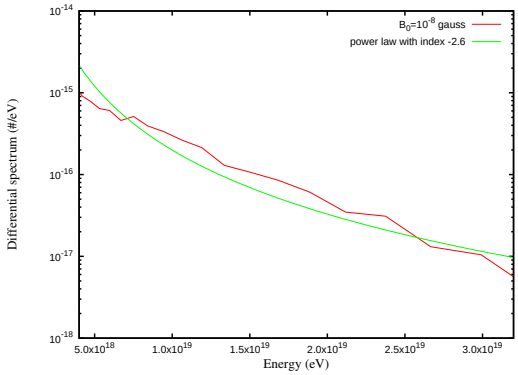

Fig. 3. Calculated differential spectrum for 1,000 protons in the energy range $\log(E/eV) = [18.6 - 19.5]$ for the selected parameters $B_0 = 10^{-8}$ gauss and $\mathcal{R} = 50$ kpc.

3 Conclusion

It is worth emphasizing that this calculation was carried out without the use of several unknown factors often required in approaches involving a hybrid Boltzmann equation to obtain the phase-space particle distribution. In addition, we point out that the acceleration mechanism we have invoked here is sustained over 10 orders of magnitude in particle energy, and the UHECRs therefore emerge naturally—without the introduction of any additional exotic physics—from the physical conditions thought to be prevalent within AGN giant radio lobes.

The importance of elucidating the mechanism of acceleration of UHECRs is confirmed by the growing number of dedicated experiments which will join Auger South: Auger North, the JEM-EUSO mission (Allard 2008), etc. The UHECR source identification will continue to improve. Eventually, we should be able to clarify whether the cutoff in the CR distribution is indeed due to propagation effects, or whether it is primarily the result of limitations in the acceleration itself. As energies as high as $\sim 10^{20}$ eV may be reached within typical radio lobes, it is possible that both of these factors must be considered in future refinements of this work.

References

Abbasi, R. U. *et al.* [HiRes Collaboration], 2008, Phys. Rev. Lett., 100, 101101
Allard, D., in these proceedings
The Auger Collaboration, 2007, Science, 318, 939
The Auger Collaboration, 2008a, Astropart. Phys. 29, 188
The Auger Collaboration, 2008b, Astropart. Phys., 29, 243
The Auger Collaboration, 2008c, Phys. Rev. Lett., 101, 061101
Bhattacharjee, P. & Sigl G. 2000, Phys. Rep., 327, 109
Bluemer, J., for the Auger Collaboration (http://arXiv.org/abs/astro-ph/0807.4871)
Cho, J., Lazarian, A., Vishniac, E.T. 2003, ApJ, 595, 812
Fermi, E. 1949, Phys. Rev., 75, 1169
Fraschetti, F. 2008, Phil. Trans. A of Royal Society, 366
Fraschetti, F., & Melia, F. 2008, Mon. Not. Roy. Astron. Soc., in press (http://arxiv.org/abs/astro-ph/0809.3686)
Gelmini, G., Kalashev, O., & Semikoz, D.V. (http://arxiv.org/abs/astro-ph/0702464)
Giacalone, J., & Jokipii, J.R. 1994, ApJ, 430, L137
Greisen, K. 1966, Phys. Rev. Lett., 16, 748
Padmanabhan, T. 2001, Theoretical Astrophysics Vol II, Cambridge University Press.
Semikoz, D. V., for the Auger Collaboration (http://arXiv.org/abs/astro-ph/0706.2960).
Torres, D.F., & Anchordoqui, L.A. 2004, Rep. Prog. Phys., 67, 1663
Verma, M.K. 2004, Phys. Rep., 401, 229
Zatsepin, G.T., & Kuz'min, V. A., 1966, Sov. J. of Exp. and Theor. Phys. Letters, 4, 78